Mechanical and Microstructural Characterization of Geopolymers from Assorted Construction and Demolition Waste-based Masonry and Glass

Hüseyin Ulugöl[1], Anıl Kul[1], Gürkan Yıldırım[2*] Mustafa Şahmaran[1], Alper Aldemir[1], Diogo Figueira[3], Ashraf Ashour[3]

[1] Department of Civil Engineering, Hacettepe University, Ankara, Turkey

[2] Department of Civil Engineering, Kırıkkale University, Kırıkkale, Turkey

[3] Department of Civil and Structural Engineering, University of Bradford, Bradford, United Kingdom

Abstract

Geopolymers are mostly produced with main-stream precursors such as fly ash and slag. These precursors are successfully used and competitively demanded by the cement industry. Development of geopolymers from alternative precursors is appealing. The main aim of this work is the development of geopolymers with construction and demolition waste-based precursors including masonry units (red clay brick, roof tile, hollow brick) and glass. Different curing temperatures (50, 65, 75, 85, 95, 105, 115, 125 ^{o}C), curing periods (24, 48, 72 h), and Na concentrations (10, 12, 15%) of alkaline activator (NaOH) were employed. Compressive strength testing and microstructural investigations were performed including X-ray diffraction, thermogravimetry and scanning electron microscopy with energy-dispersive X-ray spectroscopy. Results showed that depending on the type of precursor (hollow brick), curing temperature/period (115 ^{o}C/24 h) and concentration of alkaline activator (12%), it is possible to obtain compressive strength results more than 45 MPa. Hollow brick is the most successful precursor resulting in higher compressive strength results thanks to a more compact microstructure. The strength performance of red clay brick and roof tile is similar. The compressive strength results of geopolymers with glass precursor are lower, most probably due to significantly coarser particles of glass used. The main reaction products of red clay brick-, roof tile- and hollow brick-based geopolymers are sodium aluminosilicate hydrate (N-A-S-H) gels with zeolite-like structures while they are sodium silicate gels in the case of glass-based geopolymers. Our findings showed that CDW-based materials can be used successfully in producing geopolymers. Current research is believed to help raise awareness in novel routes for the effective utilization of such wastes which are realistically troublesome and attract further research on the utilization of CDW-based materials in geopolymer production.

***Keywords*:** Geopolymer; Construction and demolition waste (CDW); Compressive strength; Microstructure.

[*] Corresponding author. Tel: +90-318-357-1263, E-mail: gyildirim@kku.edu.tr; gurkanyildirimgy@gmail.com.

1. Introduction

Construction and demolition waste (CDW) generation has become prominent around the world, being one of the largest sectors contributing to global solid waste production. 28 member states of the European Union generated a total CDW amount of 830 million tons (Mt) in 2012, which accounts for approximately 1.65 tons per capita (Deloitte, 2017). In 2015, United States generated a total CDW amount of 548 Mt, which corresponds to nearly 1.7 tons of CDW per capita (U.S.E.P., 2018). Examples show that CDW generation is a fast-growing issue globally. Unless controlled properly, large portions of CDW will continue to flow into clean landfills and threaten the health of individuals and environment (Wang et al., 2014).

Massive concrete productions worldwide requiring high volumes of Portland cement (PC), which is well-known to has significant negative effects on the environment, push researchers seek alternative greener binders that can partially/entirely replace PC. As a possible candidate to replace PC, "geopolymers" have come to the forefront (Juenger et al., 2011). Along with their environment-friendly features, geopolymers are also reported to have superior mechanical (Neupane et al., 2018) and durability performance including resistance against acids (Thokchom et al., 2009), sulfates (Bhutta et al., 2013), alkali-silica reaction (Pouhet and Cyr, 2015) and high temperatures (Jiang et al., 2020) compared to PC-based systems.

A geopolymer is a binder obtained by the alkali-activation of a solid alumina- and silica-containing precursors (Zhang et al., 2014a). Aluminosiliceous precursors used in the production of geopolymers up to now (e.g. fly ash, blast furnace slag, calcined clays) are mostly those with already well-known properties and composition/behavior that can be continuously controlled by the manufacturer. These materials, which were formerly called by-products (e.g. fly ash, slag), are no longer regarded as waste due to their very successful and wide-spread utilization for years as pozzolanic materials in traditional concrete and blended PC production. Due to aforementioned reasons, selection of precursors for alkali-activation has broadened significantly and special attention started to be paid on materials that are not strongly demanded especially in blends with PC (Shi et al., 2019).

Studies utilizing CDW-based precursors (e.g. concrete, different types of bricks/tiles, glass) for geopolymerization have been performed thanks to the availability of CDW all over the world. Ahmari et al. (2012) produced geopolymer mixtures with the single and binary use of waste concrete powder and class F fly ash. They reported no significant strength development with the single use of waste concrete while remarkably higher compressive strength results were noted when waste concrete powder and class F fly ash were combined. Similar behavior was also noted by Vafaei and Allahverdi (2017) who tested the development of geopolymers with the combinations of calcium aluminate cement and waste glass powder and concluded

that an increase in the amount of calcium aluminate cement has enabled higher compressive strengths. Komnitsas et al. (2015) utilized concrete, brick and tile wastes as precursors in geopolymer production and stated that tiles were the best for geopolymerization reaching compressive strength of 57.8 MPa after 7 days of heat curing at 80 °C followed by 7 days of aging. In the study carried out by Robayo-Salazar et al. (2017a), CDW-based red clay brick, concrete and glass with volume-weighted mean diameters of 24, 25 and 43 μm, were used as precursors, solely or substituted with PC in producing different alkali-activated building materials. They reported that it was possible to achieve adequate mechanical properties with only CDW-based constituents, although the blends of CDW and PC resulted in better mechanical properties. Robayo-Salazar et al. (2017b) developed eco-efficient hybrid cement with the blend of alkali-activated red clay brick waste in the presence of different activators and low amount of PC (30%). They reached 28-day compressive strength result of 102 MPa. Urban ceramic waste was activated with NaOH/KOH and subjected to 28-day heat curing at 60°C in the work of Sun et al. (2013) and compressive strength of 71.1 MPa was obtained. Reig et al. (2013) used clay brick waste for alkali-activation with NaOH and reported achievement of 30 MPa compressive strength after 7-day curing at 65°C. Vázquez et al (2016) produced geopolymers activated with NaOH and water glass solution by using concrete waste singly or combined with metakaolin (10%) (hybrid) after curing at 25°C for 28 days and recorded 25 and 46 MPa compressive strengths for single and hybrid geopolymer systems. Silva et al. (2019) used fire clay brick as geopolymer precursor and looked for the optimum conditions for geopolymerization. They concluded that compressive strength of 37 MPa could be obtained with proper conditions of production (i.e. silica modulus of 0.60, Na_2O content of 8%, water-to-binder ratio of 0.27 with 7-day oven curing between 65-80°C). Ouda and Gharieb (2020) investigated the effects of incorporation of dolomite-aggregate incorporated waste concrete powder on the microstructure/strength properties of alkali-activated brick waste and reported that this incorporation has positive effects on the compressive strength results of all different-age mixtures.

Studies show that the use of CDW-based components in producing geopolymers is a hot topic requiring further attention. This is specifically important for countries troubled by CDW generation like Turkey which plans to demolish and/or reconstruct nearly 7M buildings in the next 20 years under the new infrastructure/urban transformation action and has limited competency to tackle CDW innovatively. The nature of CDW-based materials, even for similar-origin materials, changes considerably. This necessitates detailed experimental work to assess optimum material/mixture/curing parameters of CDW-based materials obtained from a certain region. Another important aspect to consider is to utilize CDW-based constituents

solely and in combination. In majority of the related studies, CDW-based constituents were used in combination with different types of pozzolanic materials and/or PC to control the behavior of ultimate geopolymer material. This is not desirable from the perspective of increased/effective CDW utilization. In the incident of construction and demolition, CDW is obtained altogether and separation of individual CDW components is costly, energy-inefficient and time-consuming.

In this study, development and characterization of geopolymer binders with the single use of CDW-based masonry (i.e. red clay brick [RCB], roof tile [RT], hollow brick [HB]) and glass (G) obtained from central Anatolian region of Turkey was investigated for the first time in literature according to authors' best knowledge. Different from most of the studies available in literature, a constant duration for the milling of different-nature CDW-based materials was applied. This is specifically important since it results in significantly different grain sizes for different-nature CDW-based materials which affects the kinetics of geopolymerization reactions although it is more viable to better represent the actual construction and demolition site cases where CDW is obtained altogether and can be less time-consuming and energy-inefficient to mill once and for all with a constant milling duration. This study also forms a basis for the planned studies of the authors which will look into the utilization of CDW-based precursors used here in different combinations to simulate the collective on-site acquirement of CDW more realistically. Production of geopolymers was made by considering different curing temperatures (50, 65, 75, 85, 95, 105, 115, 125 ^{o}C), curing periods (24, 48, 72 h), and Na concentrations (10, 12, 15%) of alkaline activator (NaOH). Performance of geopolymers was mainly characterized via compressive strength tests performed after pre-determined curing periods and further supported by microstructural characterizations including analyses of X-ray diffraction (XRD), scanning electron microscopy with energy-dispersive X-ray spectroscopy (SEM/EDX) and thermogravimetry (TG/DTG) performed by using specimens of selected mixtures.

2. Materials and Experimental Methodology

Under this section, details of CDW-based precursors and alkaline-activator used for the production of geopolymers are provided alongside with the details of mixing, proportioning, sampling and testing methods used throughout the study.

2.1 Materials

Assorted CDW-based materials including wastes of red clay brick (RCB), roof tile (RT), hollow brick (HB) and glass (G) views of which were presented in Fig. 1 were utilized singly

in producing geopolymers herein. Assorted CDW was obtained from an urban transformation area in Ankara, Turkey. These CDW-based materials were initially loaded in a hammer mill which applied primary crushing to reduce their initial size. They were then moved into a ball mill for final grinding. After crushing, similar amounts of waste materials (3.5 kg) were loaded into the ball mill at each time taking the overall capacity of the ball mill into account and milled for an hour. The configuration of ball mill (steel ball shapes/size/number) and milling duration were decided based on preliminary tests performed on clayey CDW-based materials (RCB, RT and HB) as these materials were softer than glass and no significant changes in the particle size of the clayey materials were observed, beyond an hour of milling. In literature, particle size of precursors was reported to be an important factor affecting the properties of geopolymers, and in this regard, compressive strength can be improved substantially when fractions with D_{50} < 15 μm are used (Komnitsas, et al., 2015).

Although it was presumed before milling that, for a constant duration of milling, different CDW-based materials would reach different particle sizes due to significantly different characteristics of these materials, no special attention was paid to increase the volume of finer fractions after ball milling. Keeping the milling duration constant for different CDW-based materials was made by taking into account the possibility of recycling of different types of CDW-based materials altogether for the planned future studies which would better represent the real-time cases of CDW in the actual field conditions where different types of mixed CDW are obtained collectively. Smaller particle size makes grinding significantly harder to further reduce the size of individual particles (especially glass in our case) via a procedure that requires additional steel balls with different dimensions and longer milling periods which can be more energy-inefficient, time-consuming and costly. In Fig. 2, particle size distributions of the different CDW-based precursors as obtained by laser granulometry are shown. Table 1 presents the characteristic particle diameters of the different CDW-based precursors. Table 1 and Fig. 2 point out that, compared to clayey precursors, the particle size of glass were found to be coarser after the proposed milling procedure. No further steps were taken to make glass particles finer given the previously discussed reasons.

In Table 2, chemical compositions of different CDW-based precursors as determined by X-ray fluorescence (XRF) analysis are shown. The chemical compositions of different types of bricks (RCB and HB) and roof tile (RT) were quite similar with minor differences in their oxide compositions. They were rich in siliceous and aluminous oxides which are fundamentally important for alkali-activation. On the other hand, the main oxide compositions of glass (G) which was soda-lime-based as typical to window glass were SiO_2 (73.4%), followed by Na_2O (12.8%) and CaO (10.9%).

In Fig. 3, crystalline structures of CDW-based precursors, which were analyzed with X-ray diffraction (XRD) technique are shown. Crystal compositions of different types of waste bricks were very similar despite the differences in quantities. The largest crystal composition is quartz for RCB and HB. Peaks of mullite, albite and annite were also detected in RCB and/or HB.

While RCB and HB have semi-crystalline structure, RT and G are amorphous with their broad peaks centered around approximately at 2θ values of 35° and 24°. It is well-known that glass is in amorphous state. Accordingly, waste glass used herein was found to be amorphous. RT was also in amorphous state which was not expected since the main ingredient for RT production is clay, which is in crystalline state. The amorphous structure of RT is very likely to be formed as a result of the sintering applied to clay particles at high temperatures (around 800 – 1000 °C). The sintering causes the loss of combined water in clay minerals, breaking down the crystalline clay network with silica and alumina forming a disordered amorphous phase (Reig et al., 2013).

Sodium hydroxide (NaOH) in flake form was used for alkaline activation. Composition of NaOH included a minimum 98% of sodium hydroxide, maximum 0.4% of sodium carbonate, 0.1% of sodium chloride and a maximum of 15 ppm iron. Selection of NaOH as the alkaline activator and the proposed concentrations (as will be detailed) were based on preliminary investigations made by the researchers and decided considering the effects observed on viscosity, strength grade/development of the geopolymers and cost/environmental-friendliness of the alkaline activator.

2.2 Preparation and testing of paste mixtures

During the preparation of CDW-based paste mixtures, alkali solutions were prepared initially. NaOH pellets were dissolved in tap water at different Na concentrations of 10, 12 and 15% and left in laboratory conditions to cool down until the room temperature is reached. For all paste mixtures, the water to binder ratio was 0.35. Detailed mixture proportions are provided in Table 3. No chemical admixtures were used in the mixtures to avoid any interactions that might occur with the alkali solution.

After the preparation of the alkali solutions with different Na concentrations, mixing of the pastes was started. At this phase, a selected powdery CDW-based material was poured into a mortar mixer and mixed for 60 s. Then, the alkali solution was slowly poured into the mixer and stirred for 210 s. After a 15 s waiting period during which the blade and cone of the mixer were cleaned, the paste was mixed for an additional 60 s before completion of mixing. The fresh mixtures were then cast into pre-oiled cubic molds measuring 50 mm. Immediately after molding, cubic specimens within their molds were moved into an oven for curing at different

temperatures (50, 65, 75, 85, 95, 105, 115 and 125 ^{o}C). Three different curing durations (24, 48 and 72 h) were adopted. As is well-known, current literature is quite rich in studies related to geopolymers and great variety of temperatures/durations for curing of geopolymers can be found. Different curing temperatures/durations utilized in this study were decided by taking into account the temperatures/durations utilized by different studies and overall energy requirement (Khalifeh et al., 2014). After the predetermined curing periods in the oven, specimens were taken out of the oven and immediately removed from their molds. No visible microcracks were monitored on the surfaces of the cubic specimens after curing. After cooling down to room temperature, specimens were subjected to compressive strength testing at a loading rate of 0.9 kN/s. The compressive strength results were supported with microstructural characterizations performed on some of the selected specimens obtained after compressive testing. These characterizations included X-ray diffraction (XRD) analyses, thermogravimetry (TG/DTG) and scanning electron microscopy observations with energy-dispersive X-ray spectroscopy (SEM/EDX). For an easier understanding of the experimental program/methodology, a flow diagram was constructed and presented in Fig. 4.

The XRD method is a non-destructive testing to analyze even the smallest amounts, relying on the principle of the diffraction of X-rays within a characteristic order created by atomic patterns of a specific crystalline phase of a material. This diffraction profile for each crystalline phase distinguishes a specific crystal. For the XRD analyses, the cubic geopolymer paste specimens tested for compressive strength were used and powdery samples with the approximate weight of 20 mg were obtained from crushed specimens. Crystal phase changes in the selected specimens after geopolymerization were analyzed with the help of diffractograms and compared to raw forms of CDW-based precursors.

Thermogravimetric (TG) and differential thermal analyses (DTG) were performed to obtain information from the samples exposed to temperatures ranging from 25 to 1050°C at a rate of 10 °C/min. Temperature exposure occurred in a carbon dioxide-free environment with 100 ml/min nitrogen flow. Powdery samples weighing approximately 50 mg were also obtained from some of the tested cubic geopolymer paste specimens and used in TG/DTG analyses. The amount of water loss was calculated at the end of the temperature exposure and discussed with regard to geopolymerization reactions.

Changes in the microstructures of geopolymer pastes were also analyzed with SEM/EDX. Samples taken from cubic specimens used in compressive strength testing were cut into proper dimensions (less than 1 cm in each dimension) and used for monitoring under SEM. EDX analyses were also performed to characterize the chemical formations on selected areas.

3. Results and Discussion

This section comprises of detailed discussions on the compressive strength results with regard to the effects of different curing temperatures/periods, concentration of alkaline activator and type of CDW-based precursor. It also comprises of microstructural characterization of specimens of selected mixtures with XRD, TG/DTG and SEM/EDX analyses.

3.1 Compressive strength

In Fig. 5, average compressive strength results of completely CDW-based geopolymer pastes are presented with respect to different curing temperatures, Na concentrations and curing periods. Each compressive strength result included in the plots available in Fig. 5 calculated by the averaging of the individual results obtained from three separate cubic specimens. Compressive strength results recorded from separate specimens of a known mixture were close to each other with coefficient of variation being maximum 10%. In the following sections, the effect of different mixture design parameters on the compressive strength development of geopolymer pastes is discussed separately.

3.1.1 Effect of curing temperature

Temperature is regarded to be one of the most influential parameters on the development of mechanical properties of geopolymers as it closely affects the rate of formation and quality of microstructure (Rovnaník, 2010). Fig. 5 indicates that irrespective of the curing periods, concentration of alkaline solution and type of CDW-based precursor used, the average compressive strength results showed an incremental trend for all paste mixtures with the increase in curing temperature. Depending on the alkaline solution concentration, curing temperature and type of precursor, it was possible to reach compressive strength levels exceeding 45 MPa only after 24 hours of curing (e.g. HB-based pastes with alkaline solution having 12% Na concentration and cured at 115 ºC) (Fig. 5). Based on the general process of geopolymerization, possible explanation for the increased compressive strength results at higher temperature levels can be the acceleration of initial dissolution of amorphous phases in CDW-based precursors which further triggered the processes of polycondensation and formation of hard structure (Rovnaník, 2010). In fact, what increases the dissolution rate of aluminosilicate precursors in accordance with the power-law relationship is the increased activity of hydroxide ions of alkaline solution which is significantly higher at increased temperature levels (Duxson et al., 2007). The rate of dissolution decelerates as the point of supersaturation gets closer and the process of dissolution predominantly replaces

polycondensation expelling water from the solidified gels. At this stage, dissolved phases very rapidly polymerize and reprecipitate, rearrangement/polymerization of precursors take place and some of the alkali cations (Na^+) are bonded to the aluminosilicate gel network. All of the abovementioned appears to be completed earlier when the curing temperature is higher which may lead to higher compressive strength results.

Fig. 5 shows that, at 50 ºC, which can be regarded as a moderate temperature level, there was no strength development for all pastes that were produced for the current study, regardless of different mixture parameters. Compressive strength results were recordable at curing temperature of 65 ºC or higher, although they were less than 10 MPa even at 65 ºC. It is likely that curing at lower temperatures was not adequate for the removal of unconjugated water, to sufficiently increase dissolved species for the formation of adequate amounts of aluminosilicate gels and to overcome the gelatinous and moist state of geopolymer slurries (Mo et al., 2014). Meanwhile, 50 ºC was more than enough for achieving acceptable and/or high compressive strength results for geopolymers (Mo et al., 2014). Even at ambient temperatures, reasonably high compressive strength results were easily achievable for geopolymeric materials (Nath and Sarker, 2017). It is worth mentioning that, these results of the abovementioned studies were recorded for main-stream aluminosilicate precursors with well-known properties and controlled production processes such as fly ash, ground granulated blast furnace slag and metakaolin. It may possibly be stated for the current study that due to lower purity and/or less rigorous control over the properties of CDW-based precursors, lower temperature levels might not have been as successful in achieving reasonable compressive strength results. The fineness of CDW-based precursors obtained as a result of the proposed milling method, which prioritizes less labor/energy requirement, might not also be favorable for the achievement of reasonable compressive strength results at lower temperature levels.

Incremental trend in the compressive strength results with the continuous increments in curing temperature was not valid after exceeding a certain temperature level for all geopolymers with different alkaline solution concentrations, curing periods and CDW-based precursors, indicating that there is an optimum temperature level where the largest improvements in the microstructure of geopolymers can be achieved. As Fig. 5 makes it evident, for most of the geopolymer pastes produced in this study average compressive strength results exhibited peaks when the curing temperature reached to 115 ºC. Although it was rare, compressive strength results reached maximum levels at 95 ºC or 105 ºC depending on the age, type of precursor and alkaline solution concentration for some geopolymers as well. When geopolymers are subjected to high curing temperatures (higher than the maximum temperature level which resulted in maximum compressive strength results) viscosity starts to increase

rapidly upon the commencement of polycondensation and aluminosilicate species released as a result of the dissolution of precursors are immediately captured and reacted, which leads to very fast setting of geopolymer pastes. Upon fast setting, clotting takes place in geopolymer slurry leading to coverage of the undissolved aluminosilicate precursors with geopolymeric gel. This limits the additional dissolution of amorphous phases and prevents transformation from diffluent to a hard and more compact structure. Compressive strength can also decrease at higher curing temperatures as a result of cracking at microscale and geopolymeric gel contraction caused by excessive shrinkage and dehydration (Mo et al., 2014). Another reason regarding lower compressive strength results noted at higher curing temperatures can be related to the quality of reaction products formed after geopolymerization. It is reported that when cured at lower temperatures, reaction products find enough time to slowly fill the pores available in the geopolymeric structure leading to lower porosity and higher toughness. At higher temperatures, although reactions take place very rapidly, a less ordered and more porous structure with lower-quality reaction products forms which may lower the compressive strength (Rovnaník, 2010).

3.1.2 Effect of curing periods

For a given type of precursor, alkaline solution concentration and curing temperature, extended curing periods generally increased the average compressive strength results of geopolymers (Fig. 5). It needs to be emphasized that there were certain deviations from this trend based on other geopolymer mixture parameters. The enhancement in compressive strength for most geopolymers tested was not large when curing period was increased from 48 to 72 h, suggesting that extended heat curing is not a useful tool for changing the strength results after certain period of curing as also suggested in Memon et al. (2011). The observed trend in the results with the extended curing periods can be explained with beneficial effects of heat curing on the geopolymerization reactions as explained previously.

It was interesting to note that at the optimum temperature level (115 ºC) which produced the highest compressive strength results for almost all geopolymers studied, specimens cured for shorter periods mostly resulted in higher compressive strength (Fig. 5). For example, at 115 ºC, for RT-based geopolymers produced with alkaline activator having 10% Na concentration, the average compressive strength results of specimens cured for 24, 48 and 72 h were found to be 35.5, 31.1 and 31.5 MPa. Similar observations were also valid for other geopolymer mixtures (Heah et al., 2011) and attributed to the weakening effect of longer exposure periods of elevated temperatures on the porous structure of the geopolymer mixture. It is possible that when subjected to elevated temperatures for longer periods, due to gel contraction, dehydration

and excessive shrinkage occur without transforming to a more semi-crystalline form. Longer curing periods do not affect the crystalline part of the geopolymer suggesting that amorphous phase of the gel structure is responsible for the changes in strength (Komnitsas and Zaharaki, 2007). It can be concluded that for eliminating the cracking occurrence and maintaining structural integrity, presence of certain amount of water is necessary.

3.1.3 Effect of alkaline activator concentration

The changes in the concentration of alkaline activator were one of the decisive parameters influencing the compressive strength results of geopolymers. The general trend in the average compressive strength results of geopolymers produced with NaOH solution having Na concentrations of 10, 12 and 15% is shown in Fig. 5. For a certain curing temperature/period and precursor type, increasing the Na concentration of alkaline activator from 10 to 12% resulted in increments in the compressive strength, although the results decreased after further increment in the Na concentration (15%) of the alkaline activator. To exemplify, for HB-based geopolymers cured for 24 h at 115 ºC, average compressive strengths were recorded as 43.7, 45.7 and 38.9 MPa at Na concentrations of 10, 12 and 15%. Majority of the results followed a similar trend which implied that there was an optimum Na concentration for maximizing the compressive strength results of CDW-based geopolymers (Atiş et al., 2015). As noted above, most of the proposed models for the geopolymerization constitute subsequent events of dissolution, orientation and reprecipitation of precursors and alkaline activators (Xu and van Deventer, 2000). It was stated that dissolution is the most critical event of the geopolymerization process as it plays certain roles in liberating substances that will be used in the production of SiO_4 and AlO_4 tetrahedral units and activating the surface bonding reaction (polymerization). The ultimate strength of geopolymer structure is strongly contributed by the latter (Wu and Sun, 2007). Higher compressive strength results acquired with the increment in Na concentration of alkaline activator from 10 to 12% can be related to the better ability of highly concentrated NaOH solution to dissolve the CDW-based precursors and form polymerized network having strengthened link with the dissolved particles of the precursors. On the other hand, reductions in the compressive strength results with the increment in Na concentration of alkaline activator from 12 to 15% can be attributed to coagulation of silica and faster setting which does not allow for a homogenous mixing resulting in a poor and incipient polymerization (Palomo et al., 1999). Exceeding an optimum concentration of NaOH solution also leads to electrostatic shielding, which lowers the activity of ions and impedes the dissolution of precursors causing reduction in compressive strength (Xiao et al., 2020a).

3.1.4 Effect of type of CDW-based precursor

Different precursors used in producing geopolymer pastes resulted in different compressive strength results (Fig. 5). In general, although certain variations in accordance with the other mixture parameters were observed, the highest compressive strength was noted from geopolymers produced with hollow brick (HB), while geopolymers produced with glass (G) mostly gave the lowest results. The compressive strength results of geopolymers produced with the clay-based precursors (i.e. HB, red clay brick [RCB] and roof tile [RT]), were close to each other and results well above 30 MPa were easily reachable. For instance, RCB-, RT- and HB-based geopolymers cured at 115 ºC for 24 hours resulted in 34.8, 42.3 and 45.7 MPa average compressive strength. The completeness of geopolymerization reactions in regard to different source materials can be evaluated in terms of chemical composition, solubility, particle size distribution/fineness and degree of amorphousness of precursors to a great extent. It is generally perceived that precursors characterized with a more pronounced amorphous structure, smaller particle size and high amounts of siliceous/aluminous oxides are expected to better geopolymerize. Among these parameters, there is one that seems to be the most effective. HB was the coarsest precursor compared to the other clay-based precursor materials used in this study (Table 1, Fig. 2), and also exhibited the most distinctive crystalline peaks under X-rays (Fig. 3). Yet, geopolymers with HB resulted in the highest compressive strength results. According to Komnitsas et al. (2015), when particle fractions smaller than 150 μm and D_{50} < 15 μm are used, compressive strength of geopolymers increases substantially. In the current study, even when the value of D_{50} was 27.5 μm (Table 1), very high compressive strength results were obtainable from HB-based geopolymers despite the high crystallinity of the HB, implying that although physical properties are highly important, chemical composition of the source materials is a better criterion to modify the mechanical response of geopolymers. Among all CDW-based precursors, HB has the highest total amount of SiO_2 and Al_2O_3 which are the main oxides for geopolymerization (Table 2), and are believed to be the most decisive parameter in improving the compressive strength.

Chemical composition of CDW-based precursors that are clay-originated (RCB, RT and HB) is very similar between them, (Table 2) which may lead to unclear conclusions related to the interrelationship between the chemical composition and the compressive strength results of the geopolymers. This unclarity can be accounted for by looking into the study of van Jaarsveld et al. (2003). In this study, two batches of fly ash obtained from the same source were tested for their capability of geopolymerization. The average particle sizes of these fly ashes were almost identical and their chemical compositions were quite similar with the exception of CaO being slightly higher for one of them. Despite their similarities in physical and chemical

characteristics, significant difference in setting capability of the fly ashes was observed. This difference was attributed to greater tendency of one of the fly ashes to aggregate more when introduced into aqueous media indicating the importance of surface charge of the fly ash particles on the initial setting and it was concluded that the zeta-potential of the fly ash can have an influence on the dissolution rate and setting (van Jaarsveld et al., 2003). Likewise, despite the similarities in chemical composition of the precursors, differences in compressive strength results of RCB, RT and HB may also be related to the differences in zeta-potential of these precursors.

Geopolymers produced with CDW-based glass (G) generally exhibited lower compressive strength results despite the highly amorphous nature of glass. It is more plausible to discuss the possible reasons for the lower compressive strength results in regard to the particle size distribution and chemical composition of glass. Compared to other precursors used in this study, glass is significantly coarser with nearly 40% of its grains being larger than 100 μm (Fig. 2) and the value of D_{50} being 81.3 μm. This significantly high coarseness is believed to play a critical role in the acquirement of lower strength results for geopolymers with glass. The selected environmental alkalinity and curing temperature conditions might be inadequate to attack coarser glass grains deeply. It forms products having lower binding capability and the reaction products of coarser grains may provide inadequate coating of the particles and assurance of their cohesion.

Chemical composition of glass is shown in Table 2. What differentiates glass from other CDW-based precursors is its significantly high SiO_2 (73.4%) and low Al_2O_3 (1.27%) contents. Its CaO (10.9%) and Na_2O (12.8%) contents are also higher compared to other precursors. The reductions in compressive strength results can be also related to significantly increased Si/Al ratio in geopolymers with glass. The properties of geopolymers may change substantially even with relatively small changes in Si and Al contents and increased Si/Al ratios can lead to low cross-linked aluminosilicate materials with decreased strengths (Tho-In et al., 2018). It is reported that when glass powder is solely used as the precursor, sodium silicate gel forms as the main reaction product when activated with NaOH (Redden and Neithalath, 2014). Albeit not necessarily, sodium silicate gels are reported to have higher tendency of shrinkage/cracking (Oyler, 1984) and lower stability (Redden and Neithalath, 2014), which may partly explain the lower compressive strength results. Compressive strength results are also reported to decrease at higher CaO contents as CaO consumes NaOH (Komnitsas et al., 2015). Higher Na_2O contents is expected to further increase the alkalinity of G-based geopolymers, which may also work as a strength reducing agent for the corresponding specimens as explained in Section 3.1.3. Compressive strength values as high as 36 MPa were obtainable by arranging other

mixture parameters (i.e. curing period/temperature and NaOH concentration) of geopolymer mixtures (Fig. 5). Literature studies also concluded satisfactory performance of glass incorporated geopolymer mixtures. For example, in the work of Xiao et al. (2020a), soda lime-based glass powder with D_{50} of 15.4 was used singly and in combination with Class-C fly ash at different ratios. This study concluded that with the proper arrangement of mixture composition, curing period and alkaline activator (NaOH) molarity, it was possible to obtain geopolymers with the compressive strength of nearly 35 MPa at ambient curing conditions. It was also concluded in another study that significantly high amorphous silica contents available in the waste glass powder can contribute to the formation of cementitious geopolymer gels with the help of alumina provided by Class-F fly ash available in the geopolymer system facilitating strength development (Xiao et al., 2020b).

3.2 Microstructural characterization

Under this section, the details of microstructural characterizations which include the analyses of XRD, TG/DTG and SEM/EDX are presented. Special attention was paid to specimens, which resulted in optimum compressive strength results generally.

3.2.1 X-ray diffraction (XRD)

In Fig. 6, diffractograms obtained from XRD analyses of selected specimens are presented. To be more concise, Fig. 6 only incorporated the diffractograms belonging to raw CDW-based precursors and geopolymers that were manufactured with the mixture design parameters (12% Na concentration and curing temperature/period of 115 ºC/24 hours), which generally led to the achievement of optimum compressive strength results throughout the study.

Geopolymers are amorphous under X-rays (Duxson et al., 2007), although the ultimate product is often reported to exhibit varying structure from amorphous to semi-crystalline as well (van Jaarsveld et al., 2002). A general shifting and broadening behavior was observed in the humps of precursors from 2θ of around 15-35º to 40º after reaction with NaOH solution which was reported to be typical for amorphous geopolymer gel formation (Zhang et al., 2012). For all geopolymers, except the one with glass, these humps were less visible due to high-intensity quartz peak around 27º (Zhang et al., 2014b) and other well defined peaks. After activated with the NaOH solution, the intensity of peaks of precursors either decreased substantially or transformed into almost completely different crystals, suggesting the occurrence of geopolymerization. Reductions and transformations in the peaks of precursors are expected since these minerals are used in the dissolution and reorganization steps of the geopolymerization reactions. The visible XRD peaks after geopolymerization were previously

reported (Sun et al., 2013) and was found attributable to the unreacted crystal phases feedstock of the precursors and/or formation of zeolitic structures overlapping the amorphous baseline, particularly when highly concentrated NaOH was used as the activator (Sun et al., 2013). This was further supported by Oh et al. (2010) who stated that the concentration of NaOH is decisive on the formation of different species of zeolitic reaction products. At higher concentrations of NaOH (>5M) (as in here), cancrinite ($Na_6Ca_2Al_6Si_6O_{24}(CO_3)_2$) group of minerals such as herschelite, hydroxysodalite or hydroxycancrinite (see the following paragraph below) are usually generated, which may be regarded similar to zeolite minerals in terms of the crystal structure. Likewise, earlier studies concluded that the main reaction product of alkali-activated fly ash (Palomo et al., 2004a) is sodium aluminosilicate (N-A-S-H) gel (similar to what we mainly found in the present study [see following sections]). Sodium aluminosilicate is amorphous to X-rays due to its medium- and/or long-range disorder, although it was found to exhibit zeolite-like 3-dimensional structure at nano level (Palomo et al., 2004a). According to Criado et al. (2007), this may be regarded as a confirmation that N-A-S-H gel is a zeolite precursor with a thermodynamic tendency and likely to crystallize into a zeolite which may explain the clear peaks in our study after geopolymerization.

Depending on the type, main XRD peaks of the precursors were related to quartz (SiO_2, PDF No: 96-101-1160), mullite ($Al_{2.2}Si_{0.7}O_{4.8}$, PDF No: 96-900-1568), albite ($NaAlSi_3O_8$, PDF No: 96-900-2201) and annite ($K_{0.94}Fe_{2.43}Al_{2.15}Si_{2.43}O_{12}$, PDF No: 96-900-2310) which were typical minerals for clay-originated precursors. After geopolymerization, crystal peaks related to quartz (SiO_2, PDF No: 96-101-1160), sodalite ($Na_{2.6}Al_3Si_3O_{14}Cl_{0.4}$, PDF No: 96-900-5742), cancrinite ($Na_3Ca_{0.7}Al_3Si_3O_{14}C_{0.7}$, PDF No: 96-900-4052), melilite ($Ca_{1.87}Na_{0.1}Mg_{0.96}Al_{0.09}Si_{1.98}O_7$, PDF No: 96-900-7367) and diopside ($CaMg_{0.5}Si_{1.5}O_6$, PDF No: 96-900-5281) formation were found, which were also typically reported for geopolymeric structures, as explained in Fig. 6. Among the products obtained after geopolymerization which were identifiable under X-rays, only sodalite constitutes an ion (chloride [Cl^-]) which was not available in the compositions of CDW-based precursors (Table 2, Fig. 3). Chloride ions available in the composition of sodalite are most likely to be originated from the alkaline activator (NaOH) which incorporates certain amount of sodium chloride, as noted in Section 2.1.

For RCB-based geopolymers, peaks of mullite and annite completely disappeared and peak of quartz decreased significantly after geopolymerization forming well-defined peaks of quartz, cancrinite and sodalite, which are commonly observed in alkali-activated Al-rich precursors (Provis et al., 2014). When clayey materials are overcalcined (>950 ºC), mullite crystals start to form which are reported to be unreactive in alkaline activation (Provis and

Bernal, 2014). As opposed to previous works which stated that crystalline phases (those in fly ash) such as quartz, mullite and magnetite are inalterable after alkaline activation and undergo only slight alterations (Provis and Bernal, 2014), here, quartz peaks got weaker in intensity and initial mullite peaks completely disappeared which was an outcome concordant with Palomo et al. (2004b) that stated it was possible to change the mullite crystals under strongly alkaline environments.

Fig. 6 shows that RT, as precursor, was amorphous in nature and resulted in clear crystalline peaks after geopolimerization. For RT-based geopolymers, quartz and sodalite peaks, which were higher, and melilite peaks were observed although these were weaker. Among clayey precursors, RT has the highest content of CaO with 7.42% (Table 2). Since the peaks of melilite were not that intense for RT-based geopolymer, their presence was found attributable to higher CaO content initially available in the precursor.

In the case of HB-based geopolymers, clear peaks of quartz, sodalite, cancrinite and diopside were observed. The reductions in the peaks of initial HB precursor were considerable and higher than other precursors (Fig. 6). More established and well-defined peaks of sodalite and cancrinite, together with diopside crystals were observed, all of which suggesting better and denser microstructural development and are in line with the higher compressive strength results recorded from HB-based geopolymers.

Glass precursor was amorphous, with no visible XRD peaks, and had only a broad amorphous hump. According to XRD data, reaction products of G-based geopolymers were found to be amorphous as well (Fig. 6). A very similar case was also observed in the work of Bădănoiu et al. (2015) who stated that XRD diffractograms of glass precursor and NaOH-activated geopolymers did not show any crystalline phases and maximum halo peak of glass precursors centered around 2θ of nearly 25º (which is specific for SiO_2) has shifted to higher 2θ of nearly 30º (which is specific for sodium silicate hydrates) after geopolymerization implying clear compositional changes. The shifting in the hump related to amorphous phase of glass precursors towards higher 2θ values between 29º and 31º was also reported by Torres-Carrasco and Puertas (2017) and found attributable to the increased Na_2O content in the main reaction products of glass-based geopolymers

3.2.2 Thermogravimetry (TG/DTG)

Similar to XRD analyses, CDW-based geopolymers set with the optimum compressive strength results were further investigated via thermogravimetric analyses in this section. In Fig. 7, thermogravimetry (TG) and differential thermogravimetry (DTG) curves of geopolymers

activated with NaOH solution having 12% Na concentration cured at 115 ºC for 24 hours are shown.

Fig. 7 demonstrated that the bulk of weight losses for all geopolymers took place below 200 ºC. The weight losses observed under 200 ºC are generally attributed to free water available in the trapped pores of geopolymers. Similarly, Rodríguez et al. (2013) stated that weight losses recorded under 300 ºC are related to physically bound and zeolitic water available in the reaction products, which are dominated by aluminosilicate type-gel that can be removed from the sodium/potassium silicate gel surface at these temperatures. Bernal et al. (2010) stated that it was not possible to distinguish the peaks of zeolitic reaction products by thermogravimetry since they tend to exhibit broad dehydration peak in the same temperature range attributed to loosely bound water (60-160 ºC which is very similar to the case observed here). In geopolymerization, water has a key role providing the necessary medium for dissolution of precursors and participates in hydration reactions. Upon formation and further development of geopolymeric gel, water is released back to the system (Provis and van Deventer, 2009). This is opposite to what is normally observed in traditional cementitious systems where the amount of unbound water decreases with the increment in the amount of reaction products. Higher amounts of unbound water are expected in the trapped pores when the geopolymeric gel production is higher. As such, weight losses under 200 ºC are anticipated to be higher when the amount of products increases and more unbound water is released during the geopolymer consolidation process (Autef et al., 2013). In Table 4, weight losses recorded between temperatures of 30-200 ºC and 200-1000 ºC are shown. Under 200 ºC, HB-based geopolymer sample had the highest weight loss (11.5%), while the G-based sample had the lowest (6.5%). Beyond 200 ºC, only for the HB-based geopolymer sample, a broad hump until 400 ºC was observed, which may be indicative of the evaporation of chemically bound water (Gharzouni et al., 2018). The availability of higher amounts of unbound water is attributed to two reasons: (i) – the higher extent of gel pores (micro and nano) caused by the lower density of the gel that was developed; (ii) – the higher degree of gel development via more cross-linked and organized structures, which leads to higher amounts of water to be released back to the system. In this study, consistent drops in the weight values of the geopolymers (Table 4), were mainly attributed to a higher degree of gel formation.

3.2.3 Scanning electron microscopy (SEM/EDX)

SEM micrographs were taken with EDX analyses performed on selected areas to elaborate the reaction products of different CDW-based geopolymers. In Figs. 8-11, SEM micrographs

with EDX analyses are shown for the specimens of CDW-based geopolymers activated with NaOH solution having 12% Na concentration cured at 115 ºC for 24 hours.

Significant improvements took place in the microstructures of precursors when they were subjected to geopolymerization, which can be easily monitored after comparing the SEM microstructures of precursors shown in Fig. 1 with the geopolymers shown in Figs. 8-11. Microstructural development and ultimate geopolymerization products of geopolymers were mostly in line with and supported by the previously made discussions in Section 3.2.1. Clay-based precursors were mostly well-dissolved, resulting in geopolymers with similar microstructures and geopolymerization products. Among all geopolymers analyzed, the HB-based one exhibited significantly denser and more compact microstructure with comparably less amount/size of microcracks (Fig. 10) which supported higher compressive strength results recorded from these specimens. The RCB- and RT-based geopolymers were similar in regard to their microstructures, although they were less dense with microcracks having slightly larger widths than the HB-based geopolymers. The main geopolymerization products of clay-based geopolymers (i.e. RCB, RT and HB) were found to be a mixture of N-A-S-H gels (Mahmoodi et al., 2020) with different zeolitic polytypes (e.g. sodalite, cancrinite) ranging from amorphous structure to polycrystalline, as clear peaks of Na, Al, Si were observed in EDX patterns and clear crystal-like structures were monitored in the SEM micrographs. It needs to be mentioned that slightly visible Ca peaks were observed in the EDX spectra of all clay-based geopolymers (Figs. 8-10), although their intensities were not that pronounced to have a decisive role in changing the nature of ultimate geopolymerization products (N-A-S-H gels). These Ca peaks can be related to the initial CaO contents available in the composition of precursors and formation of cancrinite, melilite and diopside as also noted in XRD results. Ca peaks with similar intensity were also monitored in the study of Mahmoodi et al. (2020) for precursor (RCB) with similar chemical composition to those of clay-based precursors used herein.

G-based geopolymers exhibited considerably less compact microstructure and the ultimate geopolymerization products were different compared to the clay-based geopolymers. Fig. 11 depicts that, glass particles were very poorly-dissolved, most probably due to their coarser particle size. Considerable amount of glass particles was found to stay intact after geopolymerization and they were only covered with a binder which seemed gelatinous in nature and had microcracks of different sorts. In EDX patterns, clear peaks of Si and Na were observed suggesting the formation of weaker sodium silicate gels as final products for G-based geopolymers which is concordant with the discussions made in the section for XRD analyses and explaining the lower compressive strength results discussed in Section 3.1. Slightly visible

Ca peaks were also observed in G-based geopolymers (Cyr et al., 2012) which was attributed to high CaO content of glass.

4. Conclusions

In this study, geopolymeric binders with CDW-based masonry units (red clay brick [RCB], roof tile [RT], hollow brick [HB]) and glass [G]) were produced. Special attention was paid to different curing temperatures/periods and concentration of alkaline activator (NaOH) solution. Analyses were made based on compressive strength tests and microstructural analyses. Results showed that increased curing temperatures increased the compressive strength of geopolymers, although results started to decrease after reaching an optimum temperature level which was mostly 115 ºC for the current study. Extended curing periods increased the compressive strength, although increments in the results were not pronounced beyond 24 hours. Increasing Na of NaOH solution from 10 to 12% increased the compressive strength while further increments up to 15% had either no or detrimental effect on the results. Among different CDW-based precursors, HB-based geopolymers resulted in the highest compressive strength results. This was mostly related to the chemical composition of HB, with higher total content of SiO_2 and Al_2O_3. The compressive strength of RCB- and RT-based geopolymers was generally similar and less than HB. G-based geopolymers gave the lowest compressive strength results under almost all conditions, possibly due to the coarser particle size and lack of Al_2O_3 in glass particles. Microstructural investigations were largely concordant with the compressive strength results For RCB-, RT- and HB-based geopolymers, main geopolymerization products were N-A-S-H gels with different zeolitic polytypes (e.g. sodalite, cancrinite) ranging from amorphous to polycrystalline structure. For G-based geopolymers, the main geopolymerization product was comparably weaker and unstable sodium silicate gels.

Declaration of competing interest

The authors declare that they have no known competing financial interests or personal relationships that could have appeared to influence the work reported in this paper.

Acknowledgements

The authors gratefully acknowledge the financial assistance of the Scientific and Technical Research Council (TUBITAK) of Turkey and British Council provided under projects: 117M447 and 218M102.

References

661 Ahmari, S., Ren, X., Toufigh, V., Zhang, L., 2012. Production of geopolymeric binder from
662 blended waste concrete powder and fly ash. Const. Build. Mater. 35, 718-29.

663 Atiş, C.D., Görür, E.B., Karahan, O., Bilim, C., İlkentapar, S., Luga, E., 2015. Very high
664 strength (120 MPa) class F fly ash geopolymer mortar activated at different NaOH amount,
665 heat curing temperature and heat curing duration. Constr. Build. Mater. 96, 673-678.

666 Autef, A., Joussein, E., Gasgnier, G., Rossignol, S., 2013. Role of the silica source on the
667 geopolymerization rate: a thermal analysis study. J. Non-Cryst. Solids. 366, 13-21.

668 Bădănoiu, A.I., Al-Saadi, T.H.A., Voicu, G., 2015. Synthesis and properties of new materials
669 produced by alkaline activation of glass cullet and red mud. Int. J. Miner. Process. 135, 1-10.

670 Bernal, S.A., de Gutierrez, R.M., Provis, J.L., Rose, V., 2010. Effect of silicate modulus and
671 metakaolin incorporation on the carbonation of alkali silicate-activated slags. Cem. Concr. Res.
672 40, 898-907.

673 Bhutta, M.A.R., Farhayu Ariffin, N., Hussin M.W., Shukor Lim, N.H.A., 2013. Sulfate and
674 sulfuric acid resistance of geopolymer mortars using waste blended ash. J. Teknol. 61, 1–5.

675 Criado, M., Fernández-Jiménez, A., De La Torre, A.G., Aranda, M.A.G., Palomo, A., 2007.
676 An XRD study of the effect of the SiO_2/Na_2O ratio on the alkali activation of fly ash. Cem.
677 Concr. Res. 37, 671-679.

678 Cyr, M., Idir, R., Poinot, T., 2012. Properties of inorganic polymer (geopolymer) mortars made
679 of glass cullet. J. Mater. Sci. 47, 2782-2797.

680 Deloitte, 2017. Study on resource efficient use of mixed wastes, improving management of
681 construction and demolition waste – Final report. Prepared for the European Commission, DG
682 ENV.

683 Duxson, P., Fernández-Jiménez, A., Provis, J.L., Lukey, G.C., Palomo, A., van Deventer,
684 J.S.J., 2007. Geopolymer technology: The current state of the art. J. Mater. Sci. 42, 2917–2933.

685 Gharzouni, A., Ouamara, L., Sobrados, I., Rossignol, S., 2018. Alkali-activated materials from
686 different aluminosilicate sources: Effect of aluminum and calcium availability. J. Non-Cryst.
687 Solids. 484, 14-25.

688 Heah, C.Y., Kamarudin, H., Al Bakri, A.M., Binhussain, M., Luqman, M., Nizar, I.K., Ruzaidi,
689 C.M., Liew, Y.M., 2011. Effect of curing profile on kaolin-based geopolymers. Phys. Procedia.
690 22, 305-311.

691 Jiang, X., Xiao, R., Zhang, M., Hu, W., Bai, Y., Huang, B., 2020. A laboratory investigation
692 of steel to fly ash-based geopolymer paste bonding behavior after exposure to elevated
693 temperatures. Constr. Build. Mater. 254, 119267.

694 Juenger, M.C.G., Winnefeld, F., Provis, J.L., Ideker, J.H., 2011. Advances in alternative
695 cementitious binders. Cem. Concr. Res. 41, 1232-1243.

696 Khalifeh, M., Saasen, A., Vralstad, T., Hodne, H., 2014. Potential utilization of class C fly ash-
697 based geopolymer in oil well cementing operations. Cem. Concr. Compos. 53, 10-17.

698 Komnitsas, K., Zaharaki, D., 2007. Geopolymerisation: A review and prospects for the
699 minerals industry. Miner. Eng. 20, 1261-1277.

700 Komnitsas, K., Zaharaki, D., Vlachou, A., Bartzas, G., Galetakis, M., 2015. Effect of synthesis
701 parameters on the quality of construction and demolition wastes (CDW) geopolymers. Adv.
702 Powder Technol. 26, 368-376.

703 Mahmoodi, O., Siad, H., Lachemi, M., Dadsetan, S., Sahmaran, M., 2020. Optimization of
704 brick waste-based geopolymer binders at ambient temperature and pre-targeted chemical
705 parameters. J. Clean. Prod. 268, 122285.

706 Memon, F.A., Nuruddin, M.F., Demie, S., Shafiq, N., 2011. Effect of curing conditions on
707 strength of fly ash-based self-compacting geopolymer concrete. Int. J. Civ. Environ. Eng. 3,
708 183-186.

709 Mo, B.H., Zhu, H., Cui, X.M., He, Y., Gong, S.Y., 2014. Effect of curing temperature on
710 geopolymerization of metakaolin-based geopolymers. Appl. Clay Sci. 99, 144-148.

711 Nath, P., Sarker, P.K., 2017. Fracture properties of GGBFS-blended fly ash geopolymer
712 concrete cured in ambient temperature. Mater. Struct. 50, 1-12.

713 Neupane, K., Chalmers, D., Kidd, P., 2018. High-strength geopolymer concrete—Properties,
714 advantages and challenges. Adv. Mater. 7, 15-25.

715 Oh, J.E., Monteiro, P.J., Jun, S.S., Choi, S., Clark, S.M., 2010. The evolution of strength and
716 crystalline phases for alkali-activated ground blast furnace slag and fly ash-based geopolymers.
717 Cem. Concr. Res. 40, 189-196.

718 Ouda, A.S., Gharieb, M., 2020. Development the properties of brick geopolymer pastes using
719 concrete waste incorporating dolomite aggregate. J Build. Eng. 27, 100919.

720 Oyler, D.C., 1984. Use of a sodium silicate gel grout for plugging horizontal methane-drainage
721 holes. Report of investigations/1984 (No. PB-84-181643; BM-RI-8843). Bureau of Mines,
722 Pittsburgh, PA (USA). Pittsburgh Research Center.

723 Palomo Á Fernández-Jiménez A, Criado M., 2004b. "Geopolymers": Same basic chemistry,
724 different microstructures. Mater. Constr. 54, 77–91.

725 Palomo, Á., Alonso, S., Fernandez-Jiménez, A., Sobrados, I., Sanz, J., 2004a. Alkaline
726 activation of fly ashes: NMR study of the reaction products. J. Am. Ceram. Soc. 87, 1141-
727 1145.

728 Palomo, A., Grutzeck, M.W., Blanco, M.T., 1999. Alkali-activated fly ashes: a cement for the
729 future. Cem. Concr. Res. 29, 1323-1329.

730 Pouhet, R., Cyr, M., 2015. Alkali–silica reaction in metakaolin-based geopolymer mortar.
731 Mater. Struct. 48, 571-583.

732 Provis J.L., van Deventer J.S.J., 2009. Geopolymers: Structures, Processing, Properties and
733 Industrial Applications, first ed. Elsevier, Woodhead, Cambridge, UK.

734 Provis, J. L., Bernal, S. A., 2014. Geopolymers and related alkali-activated materials. Annu.
735 Rev. Mater. Res. 44, 299-327.

736 Provis, J.L., Fernández-Jiménez, A., Kamseu, E., Leonelli, C., Palomo, A., 2014. Binder
737 chemistry – Low-calcium alkali-activated materials, Alkali Activated Materials. RILEM State-
738 of-the-Art Reports, Springer, Dordrecht.

739 Redden, R., Neithalath, N., 2014. Microstructure, strength, and moisture stability of alkali
740 activated glass powder-based binders. Cem. Concr. Compos. 45, 46-56.

741 Reig, L., Tashima, M.M., Borrachero, M.V., Monzó, J., Cheeseman, C.R., Payá, J., 2013.
742 Properties and microstructure of alkali-activated red clay brick waste. Const. Build. Mater. 43,
743 98-106.

744 Robayo-Salazar, R.A., Mejía-Arcila, J.M., de Gutiérrez, R.M., 2017b. Eco-efficient alkali-
745 activated cement based on red clay brick wastes suitable for the manufacturing of building
746 materials. J. Clean. Prod. 166, 242-252.

747 Robayo-Salazar, R.A., Rivera, J.F., de Gutiérrez, R.M., 2017a. Alkali-activated building
748 materials made with recycled construction and demolition wastes. Const. Build. Mater. 149,
749 130-138.

Rodríguez, E.D., Bernal, S.A., Provis, J.L., Paya, J., Monzo, J.M., Borrachero, M.V., 2013. Effect of nanosilica-based activators on the performance of an alkali-activated fly ash binder. Cem. Concr. Compos. 35, 1-11.

Rovnaník, P., 2010. Effect of curing temperature on the development of hard structure of metakaolin-based geopolymer. Constr. Build. Mater. 24, 1176–1183.

Shi, C., Qu, B., Provis, J.L., 2019. Recent progress in low-carbon binders. Cem. Concr. Res. 122, 227-250.

Silva, G., Castañeda, D., Kim, S., Castañeda, A., Bertolotti, B., Ortega-San-Martin, L., Nakamatsu, J., Aguilar, R., 2019. Analysis of the production conditions of geopolymer matrices from natural pozzolana and fired clay brick wastes. Const. Build. Mater. 215, 633-643.

Sun, Z., Cui, H., An, H., Tao, D., Xu, Y., Zhai, J., Li, Q., 2013. Synthesis and thermal behavior of geopolymer-type material from waste ceramic. Const. Build. Mater. 49, 281-287.

Tho-In, T., Sata, V., Boonserm, K., Chindaprasirt, P., 2018. Compressive strength and microstructure analysis of geopolymer paste using waste glass powder and fly ash. J. Clean. Prod. 172, 2892-2898.

Thokchom, S., Ghosh, P., Ghosh, S., 2009. Acid resistance of fly ash based geopolymer mortars. Int. J. Rec. Trends Eng. Tecnol. 1, 36-40.

Torres-Carrasco, M., Puertas, F., 2017. Waste glass as a precursor in alkaline activation: Chemical process and hydration products. Constr. Build. Mater. 139, 342-354.

U.S.E.P. Agency Office of Resource Conservation and Recovery, 2018. Construction and demolition debris generation in the United States.

Vafaei, M., Allahverdi, A., 2017. High strength geopolymer binder based on waste-glass powder. Adv. Powder Technol. 28, 215-222.

Van Jaarsveld, J.G.S., van Deventer, J.S.J., Lukey, G.C., 2003. The characterisation of source materials in fly ash-based geopolymers. Mater. Lett. 57, 1272-1280.

Vásquez, A., Cárdenas, V., Robayo, R.A., de Gutiérrez, R.M., 2016. Geopolymer based on concrete demolition waste. Adv. Powder Technol. 27, 1173-1179.

Wang, J., Li, Z., Tam, V.W.Y., 2014. Critical factors in effective construction waste minimization at the design stage: A Shenzhen case study. China, Resour. Conserv. Recycl. 82, 1-7.

Wu, H.C., Sun, P., 2007. New building materials from fly ash-based lightweight inorganic polymer. Constr. Build. Mater. 21, 211–217.

Xiao, R., Ma, Y., Jiang, X., Zhang, M., Zhang, Y., Wang, Y., Huang, B., He, Q., 2020a. Strength, microstructure, efflorescence behavior and environmental impacts of waste glass geopolymers cured at ambient temperature. J. Clean. Prod. 252, 119610.

Xiao, R., Polaczyk, P., Zhang, M., Jiang, X., Zhang, Y., Huang, B., Hu, W., 2020b. Evaluation of glass powder-based geopolymer stabilized road bases containing recycled waste glass aggregate. Transp. Res. Rec. 2674, 22-32.

Xu, H., van Deventer, J.S.J., 2000. The geopolymerisation of alumino-silicate minerals. Int. J. Miner. Process. 59, 247-266.

Zhang, M., El-Korchi, T., Zhang, G., Liang, J., Tao, M., 2014b. Synthesis factors affecting mechanical properties, microstructure, and chemical composition of red mud–fly ash based geopolymers. Fuel. 134, 315-325.

Zhang, Z., Provis, J.L., Reid, A., Wang, H., 2014a. Geopolymer foam concrete: An emerging material for sustainable construction. Constr. Build. Mater. 56, 113-127.

Zhang, Z., Wang, H., Provis, J.L., Bullen, F., Reid, A., Zhu, Y., 2012. Quantitative kinetic and structural analysis of geopolymers. Part 1. The activation of metakaolin with sodium hydroxide. Thermochim. Acta. 539, 23-33.

Nomenclature

Abbreviation	**Full Name**
XRD	X-ray Diffraction
SEM	Scanning Electron Microscopy
EDX	Energy Dispersive Spectroscopy
TG	Thermogravimetry
DTG	Derivative Thermogravimetry
PC	Portland Cement
CDW	Construction and Demolition Waste
RT	Roof Tile

HBW	Hollow Brick
RCB	Red Clay Brick
G	Glass
PDF	Powder Diffraction File
N-A-S-H	Sodium Alumino Silicate Hydrate
D_{10}	The portion of particles with diameters smaller than this value is 10%
D_{50}	The portion of particles with diameters smaller than this value is 50%
D_{90}	The portion of particles with diameters smaller than this value is 90%
$D_{3,2}$	Surface-Weighted Mean Diameter
$D_{4,3}$	Volume-Weighted Mean Diameter

List of Tables and Figures

Fig. 1. Different assorted CDW-based precursors (starting from left to right in the direction of arrows): at raw state, after crushing, after grinding and under scanning electron microscope.

Fig. 2. Particle size distributions of CDW-based precursors.

Fig. 3. X-ray diffractograms of CDW-based precursors.

Fig. 4. A flow diagram of overall experimental program/methodology of the study.

Fig. 5. Changes in average compressive strength results of completely CDW-based geopolymer pastes with respect to different mixture parameters.

Fig. 6. XRD diffractograms of CDW-based precursors and geopolymers activated with NaOH solution having 12% Na concentration cured at 115 ºC for 24 hours.

Fig. 7. Thermogravimetry/differential thermogravimetry (TG/DTG) curves of CDW-based geopolymers activated with NaOH solution having 12% Na concentration cured at 115 ºC for 24 hours (dashed and straight curves represent the TG and DTG results).

Fig. 8. SEM micrographs with EDX spectra of RCB-based geopolymer activated with NaOH solution having 12% Na concentration cured at 115 ºC for 24 hours.

Fig. 9. SEM micrographs with EDX spectra of RT-based geopolymer activated with NaOH solution having 12% Na concentration cured at 115 ºC for 24 hours.

Fig. 10. SEM micrographs with EDX spectra of HB-based geopolymer activated with NaOH solution having 12% Na concentration cured at 115 ºC for 24 hours.

Fig. 11. SEM micrographs with EDX spectra of G-based geopolymer activated with NaOH solution having 12% Na concentration cured at 115 ºC for 24 hours.

Table 1 Characteristic particle diameters of different CDW-based precursors (units are in μm).

CDW-based material	Surface-weighted mean diameter ($D_{3,2}$)	Volume-weighted mean diameter ($D_{4,3}$)	D_{10}	D_{50}	D_{90}
Red clay brick (RCB)	2.9	16.4	1.2	7.6	46.9
Hollow brick (HB)	4.7	82.0	1.8	27.5	246.7
Roof tile (RT)	3.9	44.4	1.5	18.3	94.6
Glass (G)	16.9	111.9	7.5	81.3	263.6

865 **Table 2** Chemical compositions of CDW-based precursors.

Chemical composition, %	Red clay brick (RCB)	Roof tile (RT)	Hollow brick (HB)	Glass (G)
Loss on ignition	2.18	2.11	1.99	0.29
SiO_2	53.4	54.0	61.6	73.4
Al_2O_3	20.5	15.9	17.3	1.27
Fe_2O_3	7.77	8.93	6.70	0.18
CaO	4.75	7.42	3.31	10.9
MgO	3.70	4.84	2.66	0.18
SO_3	1.16	0.68	0.38	0.10
Na_2O	1.53	1.41	1.61	12.8
K_2O	3.42	2.30	2.80	0.08
TiO_2	1.02	1.19	0.81	0.07
P_2O_5	0.18	0.23	0.18	-
Cr_2O_3	0.04	0.04	0.03	0.02
Mn_2O_3	0.13	0.16	0.11	0.01

866
867
868 **Table 3** Proportions of the completely CDW-based paste mixtures.

CDW-based precursor (450 g)	Alkaline solution				Water-to-binder ratio	Alkaline activator-to-binder ratio
	Na		NaOH (g)	Water (g)		
	%	Molarity (M)				
Red clay brick (RCB)	10	12.4	78.3	139.9	0.35	0.48
	12	14.9	93.9	136.4	0.35	0.51
	15	18.6	117.4	131.1	0.35	0.55
Roof tile (RT)	10	12.4	78.3	139.9	0.35	0.48
	12	14.9	93.9	136.4	0.35	0.51
	15	18.6	117.4	131.1	0.35	0.55
Hollow brick (HB)	10	12.4	78.3	139.9	0.35	0.48
	12	14.9	93.9	136.4	0.35	0.51
	15	18.6	117.4	131.1	0.35	0.55
Glass (G)	10	12.4	78.3	139.9	0.35	0.48
	12	14.9	93.9	136.4	0.35	0.51
	15	18.6	117.4	131.1	0.35	0.55

869
870
871 **Table 4** Weight losses of CDW-based geopolymers during TG/DTG analyses under different
872 temperature ranges.

CDW-based geopolymer	**Temperature range**	
	30-200 ºC	**200-1000 ºC**
Red clay brick (RCB)	10.0%	5.7%
Roof tile (RT)	9.7%	6.1%
Hollow brick (HB)	11.5%	6.9%
Glass (G)	6.5%	6.8%

873

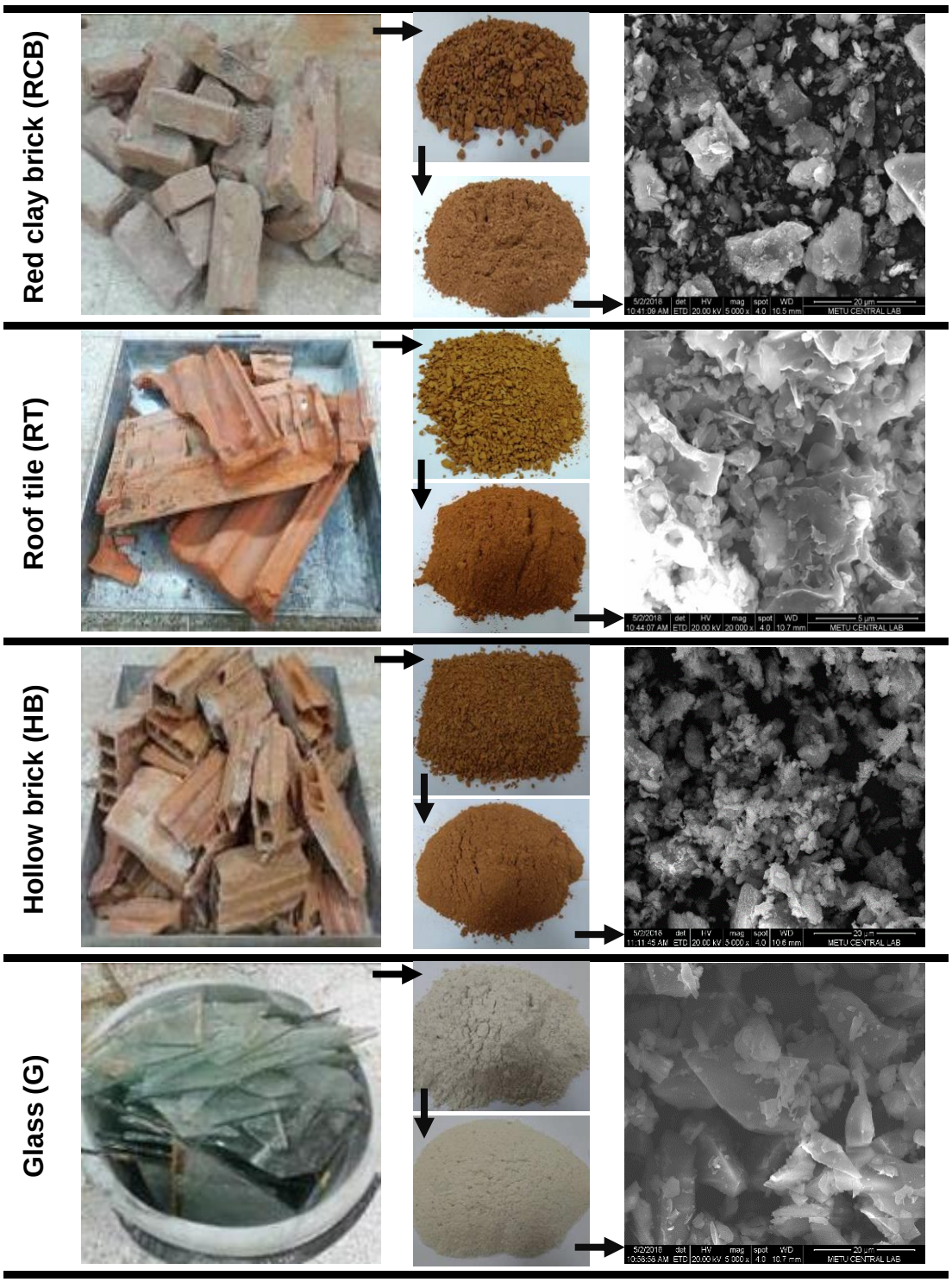

874 **Fig. 1.** Different assorted CDW-based precursors (starting from left to right in the direction of
875 arrows): at raw state, after crushing, after grinding and under scanning electron microscope.

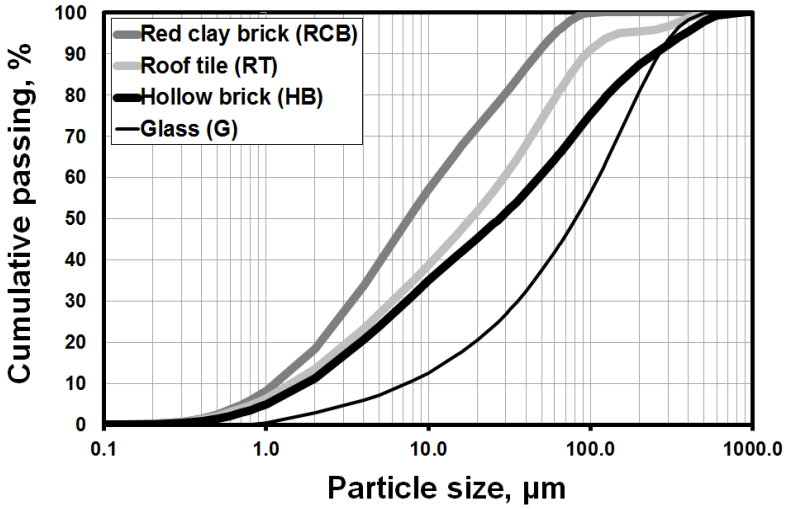

Fig. 2. Particle size distributions of CDW-based precursors.

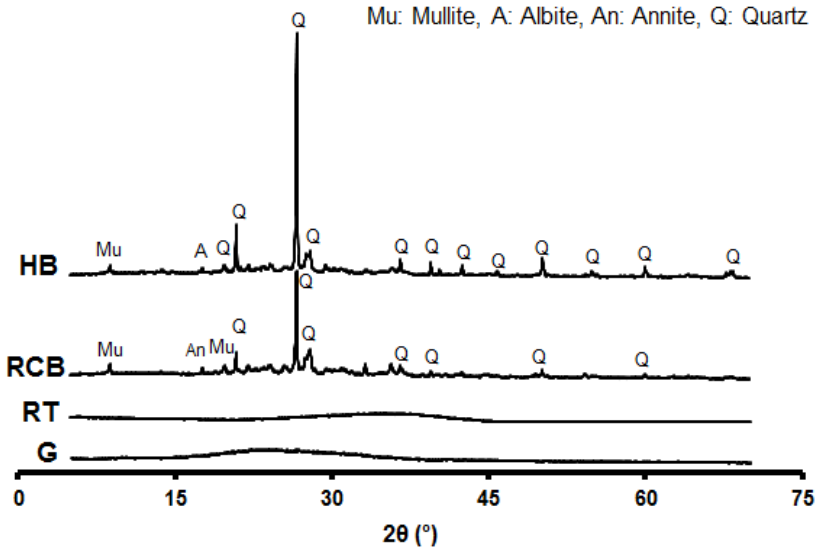

Fig. 3. X-ray diffractograms of CDW-based precursors (Powder diffraction file [PDF] numbers: Mullite ($Al_{2.2}Si_{0.7}O_{4.8}$) PDF No: 96-900-1568, Albite ($NaAlSi_3O_8$) PDF No: 96-900-2201, Annite ($K_{0.94}Fe_{2.43}Al_{2.15}Si_{2.43}O_{12}$) PDF No: 96-900-2310, Quartz (SiO_2) PDF No: 96-101-1160.

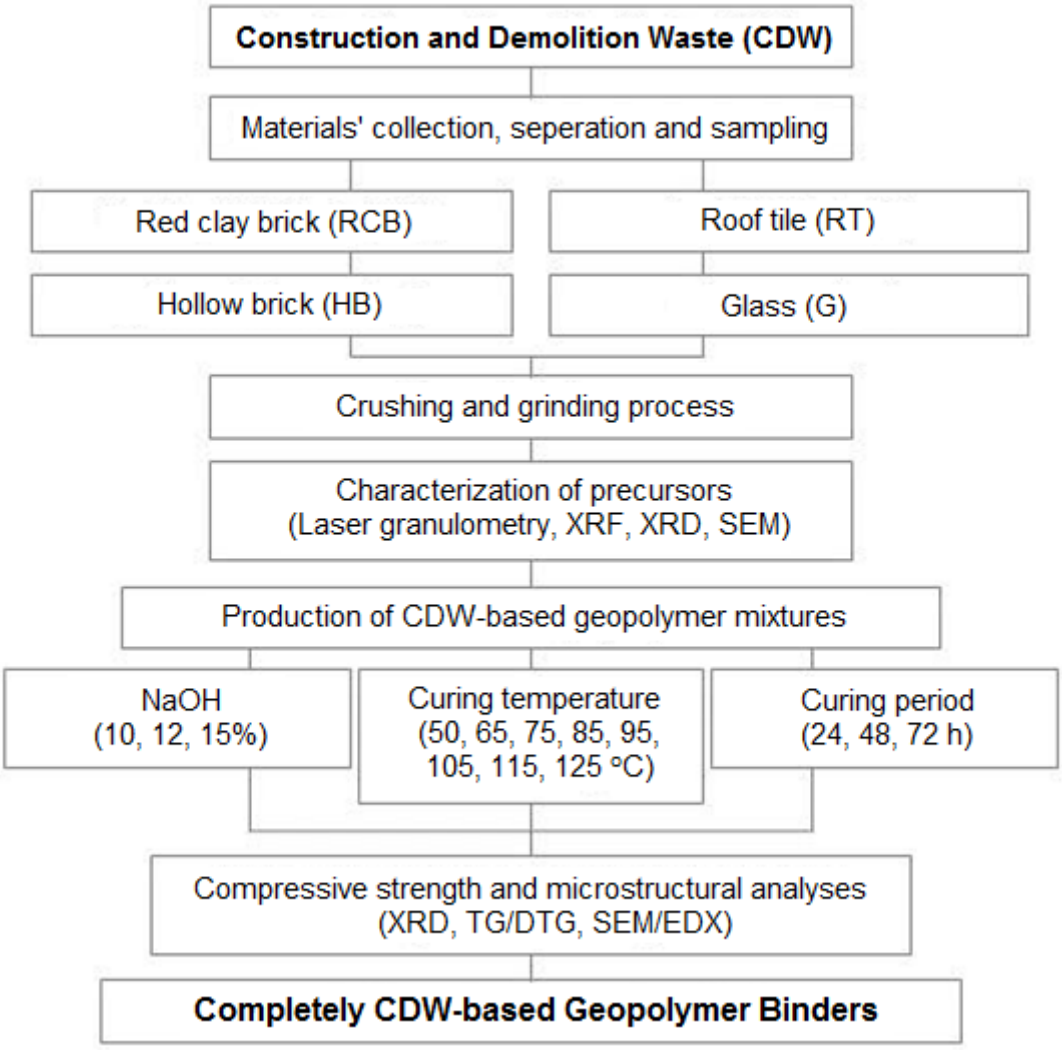

Fig. 4. A flow diagram of overall experimental program/methodology of the study.

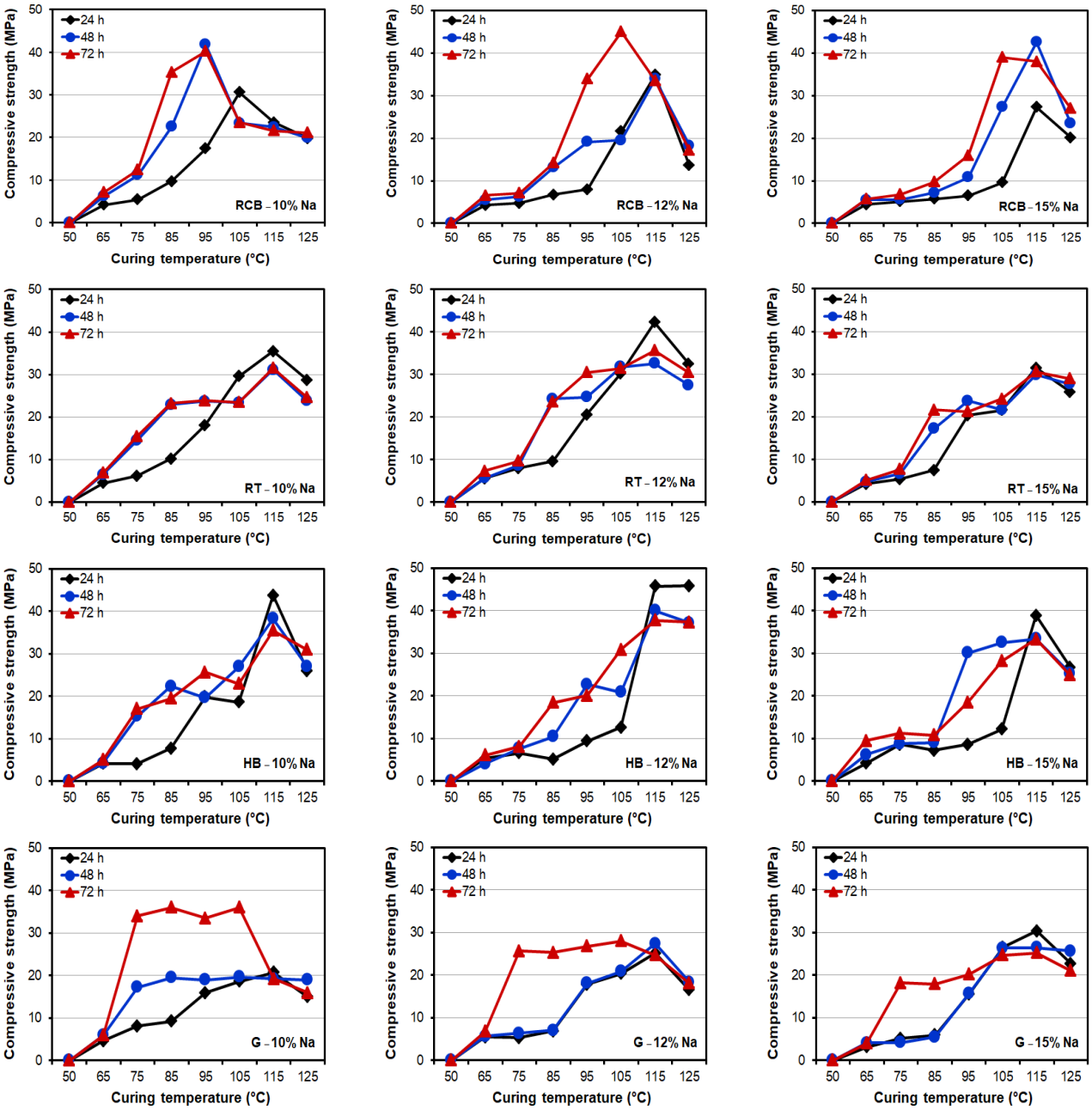

Fig. 5. Changes in average compressive strength results of completely CDW-based geopolymer pastes with respect to different mixture parameters.

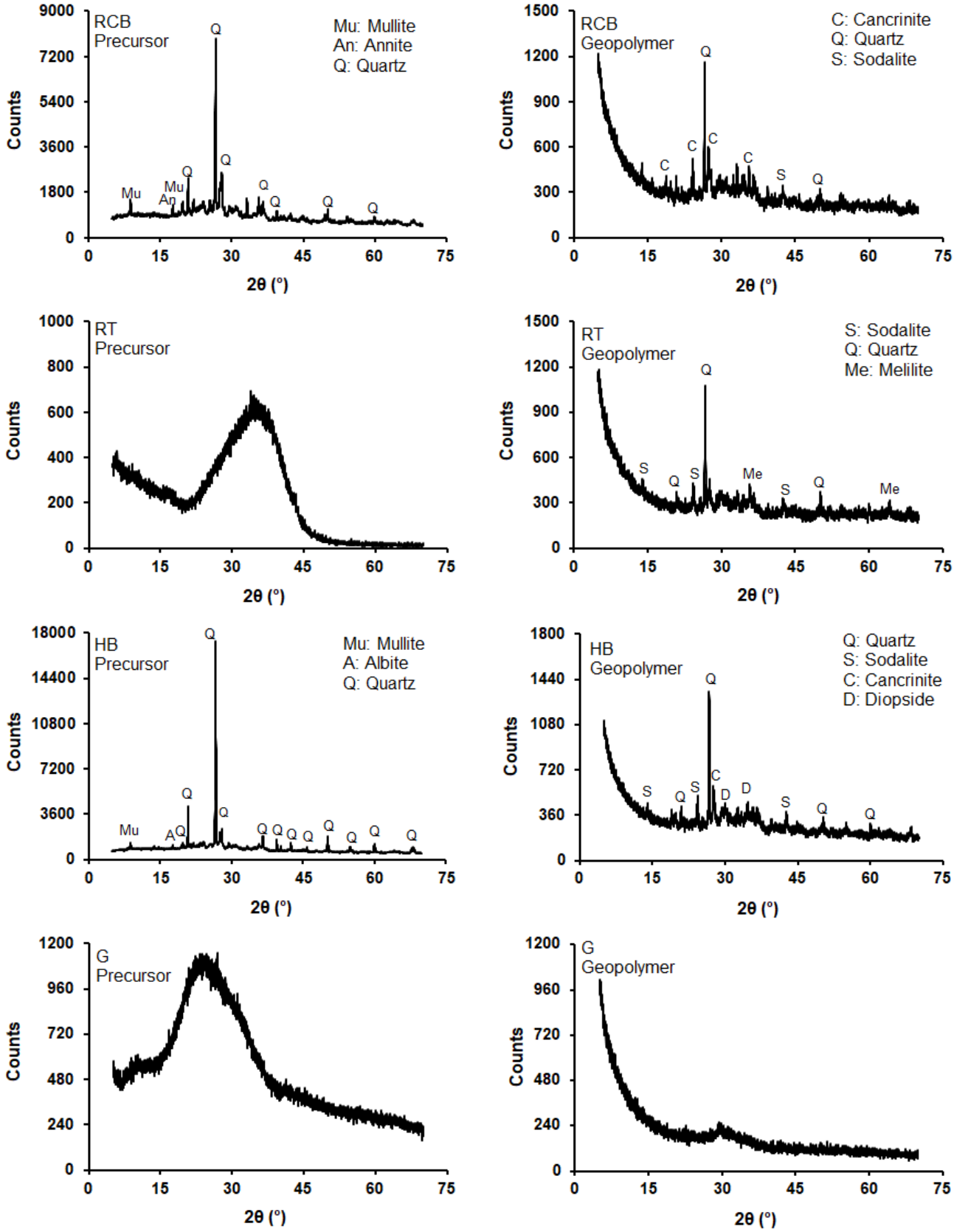

Fig. 6. XRD diffractograms of CDW-based precursors and geopolymers activated with NaOH solution having 12% Na concentration cured at 115 ºC for 24 hours. Cancrinite ($Na_3Ca_{0.7}Al_3Si_3O_{14}C_{0.7}$) PDF No: 96-900-4052, Quartz (SiO_2) PDF No: 96-101-1160, Sodalite ($Na_{2.6}Al_3Si_3O_{14}Cl_{0.4}$) PDF No: 96-900-5742, Melilite ($Ca_{1.87}Na_{0.1}Mg_{0.96}Al_{0.09}Si_{1.98}O_7$) PDF No: 96-900-7367, Diopside ($CaMg_{0.5}Si_{1.5}O_6$) PDF No: 96-900-5281.

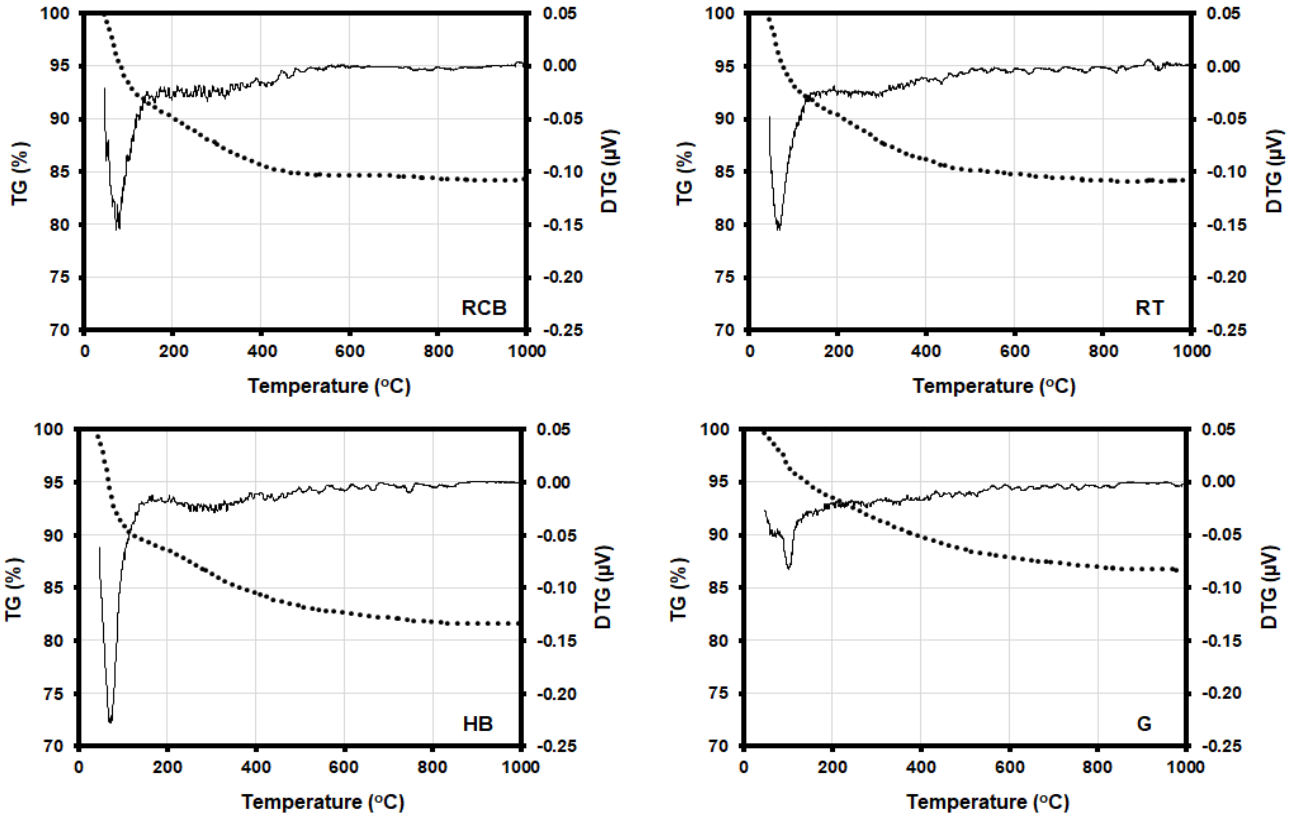

Fig. 7. Thermogravimetry/differential thermogravimetry (TG/DTG) curves of CDW-based geopolymers activated with NaOH solution having 12% Na concentration cured at 115 °C for 24 hours (dashed and straight curves represent the TG and DTG results).

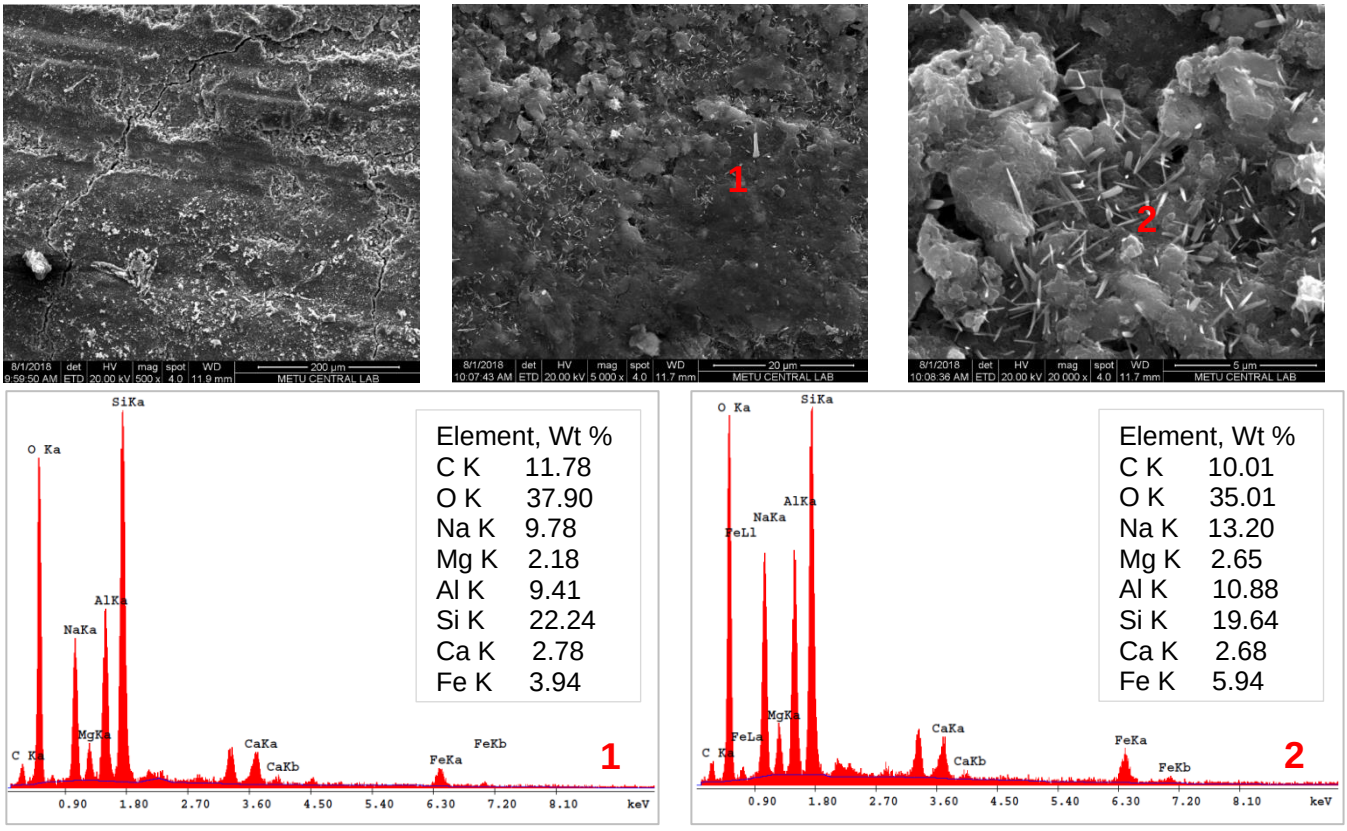

Fig. 8. SEM micrographs with EDX spectra of RCB-based geopolymer activated with NaOH solution having 12% Na concentration cured at 115 °C for 24 hours.

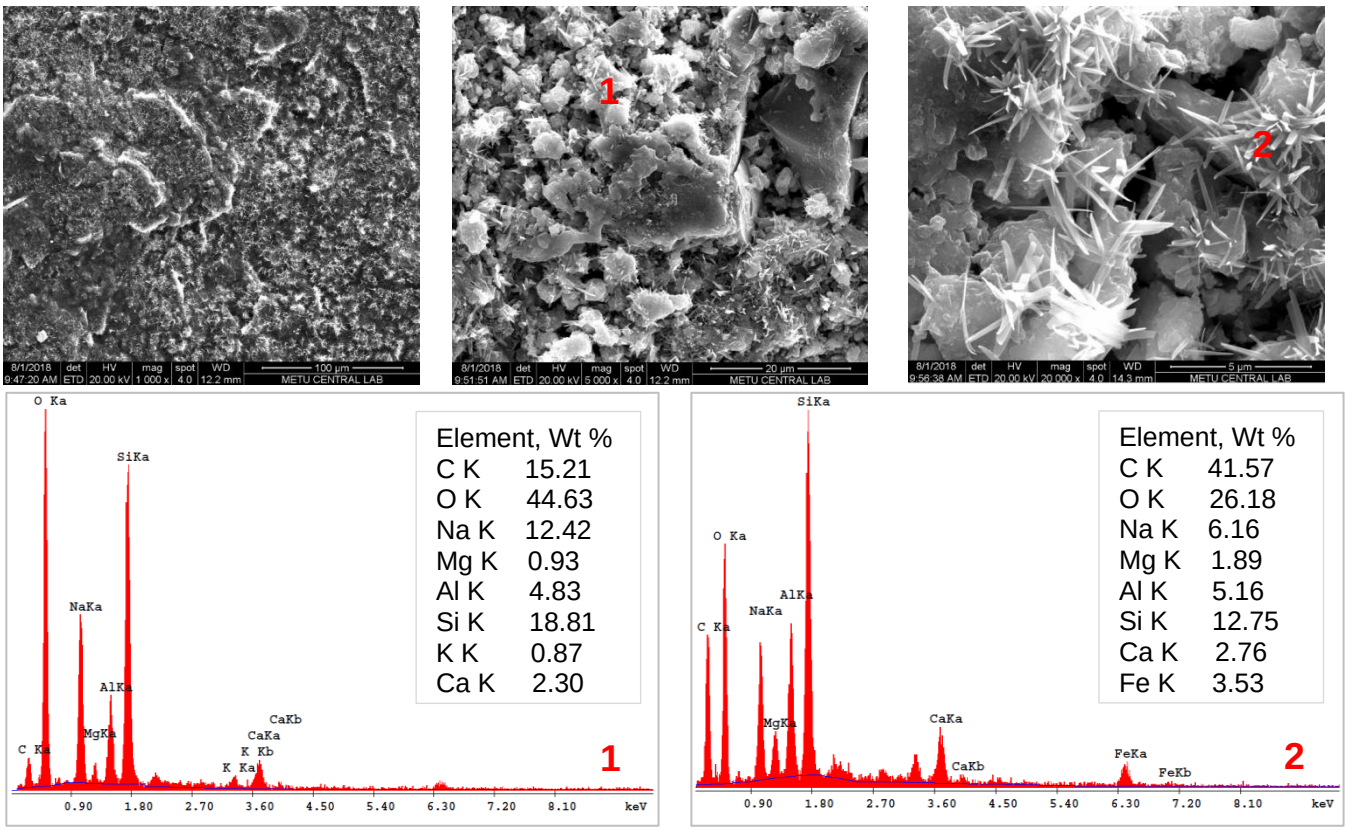

939 **Fig. 9.** SEM micrographs with EDX spectra of RT-based geopolymer activated with NaOH
940 solution having 12% Na concentration cured at 115 ºC for 24 hours.
941
942

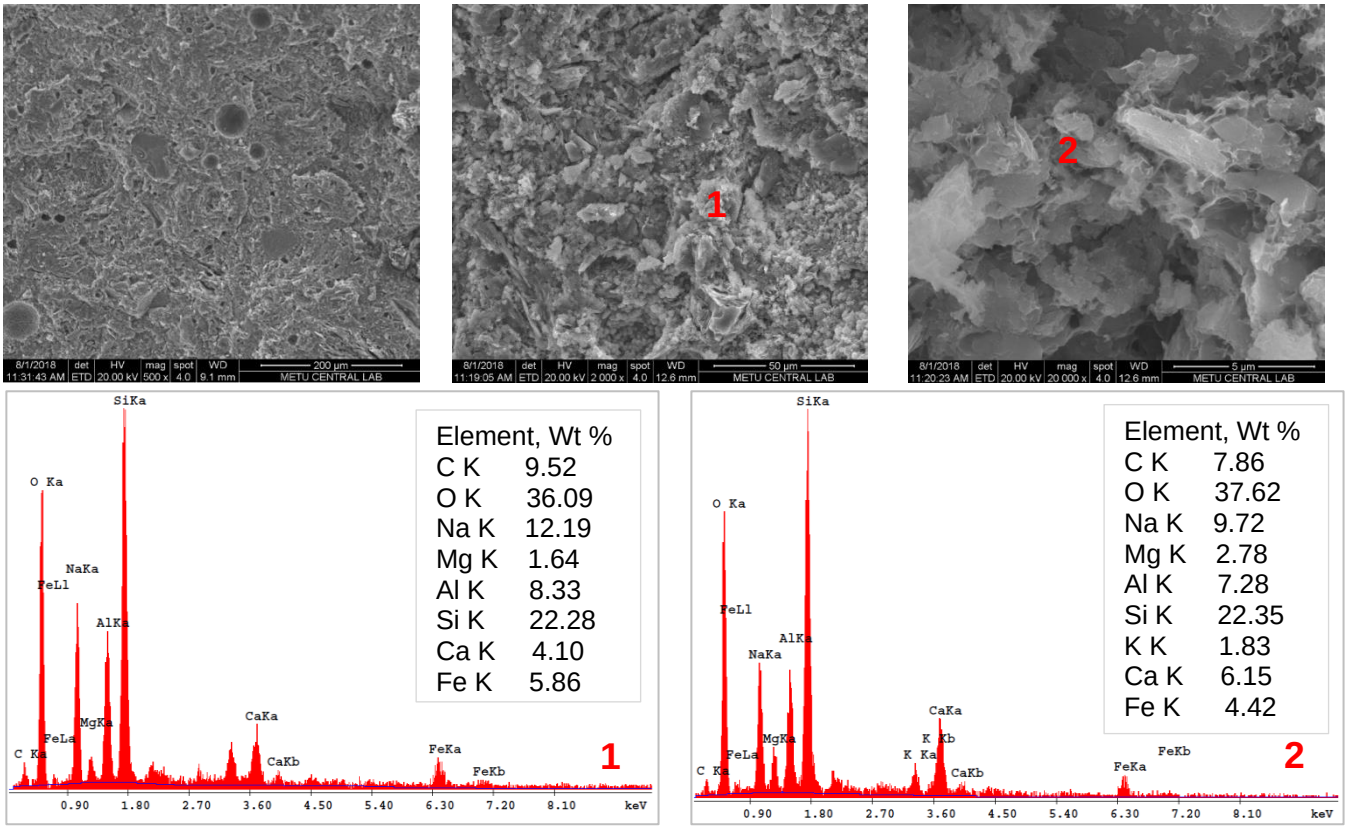

943 **Fig. 10.** SEM micrographs with EDX spectra of HB-based geopolymer activated with NaOH
944 solution having 12% Na concentration cured at 115 ºC for 24 hours.

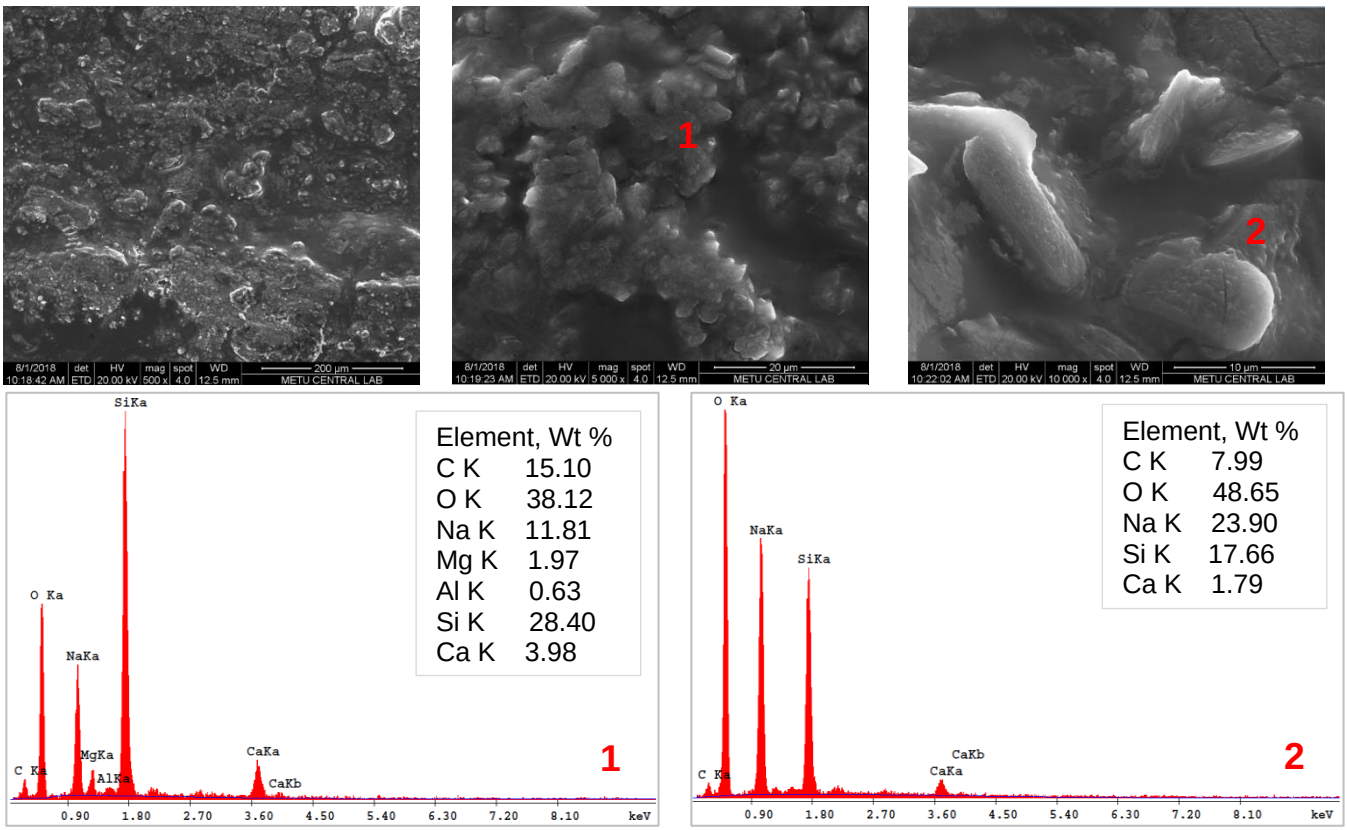

945 **Fig. 11.** SEM micrographs with EDX spectra of G-based geopolymer activated with NaOH
946 solution having 12% Na concentration cured at 115 ºC for 24 hours.